Far infrared optical properties of the pyrochlore spin ice compound $Dy_2Ti_2O_7$

2005 J. Phys.: Condens. Matter 17 5225

(http://iopscience.iop.org/0953-8984/17/34/007)

INSTITUTE OF PHYSICS PUBLISHING JOURNAL OF PHYSICS: CONDENSED MATTER

J. Phys.: Condens. Matter **17** (2005) 5225–5233 doi:10.1088/0953-8984/17/34/007

Far infrared optical properties of the pyrochlore spin ice compound $Dy_2Ti_2O_7$

C Z Bi[1,2], J Y Ma[1], B R Zhao[1], Z Tang[2], D Yin[2], C Z Li[2], D Z Yao[2], J Shi[2] and X G Qiu[1]

[1] National Laboratory for Superconductivity, Institute of Physics, Chinese Academy of Sciences, PO Box 603, Beijing 100080, People's Republic of China
[2] Department of Physics, Wuhan University, Wuhan, Hubei 430072, People's Republic of China

Received 8 June 2005, in final form 26 July 2005
Published 12 August 2005
Online at stacks.iop.org/JPhysCM/17/5225

Abstract

Near normal incidence far infrared reflectivity spectra of [111] dysprosium titanate ($Dy_2Ti_2O_7$) single crystal have been measured at different temperatures. Seven phonon modes (eight at low temperature) are identified at frequencies below 1000 cm^{-1}. Optical conductivity spectra are obtained by fitting all the reflectivity spectra with the factorized form of the dielectric function. Both the Born effective charges and the static optical permittivity are found to increase with decreasing temperature. Moreover, phonon linewidth narrowing and a phonon mode shift with decreasing temperature are also observed, which may result from enhanced charge localization. The redshift of several low frequency modes is attributed to the spin–phonon coupling. All observed optical properties can be explained within the framework of the nearest neighbour ferromagnetic (FM) spin ice model.

1. Introduction

Recently, there has been a surge of interest in the properties of the pyrochlore compound $Dy_2Ti_2O_7$, which is considered to be a model 'spin ice' material. 'Spin ice' materials, governed by the same statistical mechanics of the so-called 'ice rule' as the hydrogen atoms in the ground state of ordinary hexagonal ice I_h, have macroscopically degenerate ground states down to almost zero temperature [1–9]. Experimentally, the observed value of $(1/2)R\ln(3/2)$ found through specific heat measurement [1] is consistent with what is expected from Pauling's theory, while the spin entropy only freezes out below about 4 K [2]. From magnetic susceptibility studies, a strongly frequency dependent cooperative spin freezing is observed at about 16 K, which is associated with a very narrow distribution of spin relaxation times and a sharp drop at about 2 K [3, 6]. Neutron scattering studies performed by Fennell *et al* [4] also demonstrate well the spin ice state and the coexistence of long range ferromagnetic and short range antiferromagnetic order in a magnetic field applied along the [110] axis of $Dy_2Ti_2O_7$. As regards the theoretical aspect, Melko and co-workers [7] report numerical results on the

low temperature properties of the dipolar spin ice model obtained by the multicanonical Monte Carlo (MC) method and they find a first-order transition to a long range ordered phase. Other researchers [8] also confirm the existence of the transition under a magnetic field along the [110] axis with MC simulation.

$Dy_2Ti_2O_7$ has a typical $A_2B_2O_7$ structure with the space group $Fd3m$ (O_h^7), No 227. The B cation is sixfold coordinated and locates at the centre of the distorted octahedron formed by corner O ions. The A-site ions, i.e., Dy^{3+} (magnetic rare-earth ions with effective spin $S = 1/2$), reside on a lattice of corner-sharing tetrahedra, as shown in figure 1 of [3]. In the Dy^{3+} sublattice topology the spin configuration with two spins pointing directly towards while two spins pointing directly away from the centre of the tetrahedra corresponds to the analogous proton disorder in real ice. Then a ferromagnetic and dipolar nearest neighbour spin–spin interaction leads to a strong geometrical frustration, preventing the system from undergoing long range ordering. As a result, high degeneracy of spin states will occur at low temperature.

Owing to the Ising anisotropy arising from the crystal field effect in the pyrochlore lattice, the macroscopically degenerate states when the field is along the [111] direction are different from those for other field directions. For the [111] direction, the frustration structure changes from that of a three-dimensional pyrochlore to that of a two-dimensional Kagome-like lattice with constraint, leading to different values of the zero-point entropy [5]. The combination of ferromagnetic coupling and Ising anisotropy may be a reason for the strong frustration. But how the spins interact with each other is not well understood for the spin ice materials.

Up to now, there has been no experimental report on the infrared optical properties of $Dy_2Ti_2O_7$. IR spectroscopy can give insight into the dynamical processes related to phonons, charge carriers and spins. Motivated by this situation, we studied the infrared reflectivity of $Dy_2Ti_2O_7$ single crystal on the [111] plane from room temperature down to 10 K. The temperature dependence of the phonon modes is obtained, and the role played by spin–phonon coupling in the phonon modes is discussed.

2. Experimental details

$Dy_2Ti_2O_7$ single crystal was prepared by the floating zone method, using an infrared furnace equipped with two elliptical mirrors. Before the single-crystal growth, the polycrystalline rods were prepared by standard solid state reaction. A stoichiometric mixture of Dy_2O_3 (CERAC, 99.99%) and TiO_2 (CERAC, 99.9%) was heated in air at 1250 °C for five days with intermediate regrinding to ensure complete reaction. The typical growth condition was 4.5 mm h^{-1} for both feed and growth speeds. To avoid oxygen deficiency, the single crystal was grown in an O_2 atmosphere of 0.3 MPa. The single crystal obtained was translucent yellow. Powder x-ray diffraction measurements on the crystal confirmed that the product was single phase with cubic pyrochlore structure and the parameter of the unit cell was $a = 10.1122$ Å. The principal axes were determined using the Laue diffraction pattern.

The crystal was cleaved and one-side polished with the surface parallel to the [111] plane. The reflectivity spectra $R(\omega)$ at different temperatures were measured at near normal incidence of about 8° using a Bomen DA8 Fourier transform infrared spectrometer, in the range from 50 to 6500 cm^{-1}. In the far infrared region, a He cooled bolometer and 6 mm Mylar beam splitter were used. In the middle infrared region, a liquid nitrogen cooled mercury cadmium telluride detector and KBr beam splitter were utilized. For obtaining the absolute reflectivity, an evaporated gold mirror served as a reference. Spectra were collected with a resolution of 4 cm^{-1}. The samples were mounted in a continuous helium flow cryostat in which the temperature could be varied between 300 and 10 K.

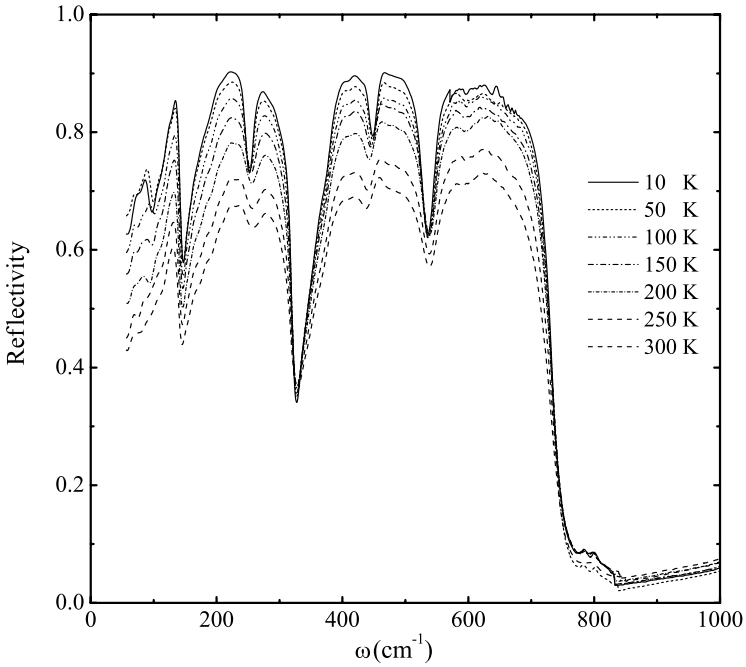

Figure 1. The temperature dependence of the reflectance of $Dy_2Ti_2O_7$ single crystal in the range of 50–1000 cm^{-1}.

3. Results and discussion

The temperature dependent reflectivity of the $Dy_2Ti_2O_7$ single crystal shown in figure 1 is typical for a nonmetallic system. The sharp features in the reflectivity spectra are due to the unscreened infrared active optical phonon modes; above the highest observed lattice vibration frequency, the reflectivity is flat and featureless up to the highest measured frequency. It can be seen that the reflectivity within the reststrahlen bands increases with decreasing temperature. At high temperature seven modes can easily be identified.

The mode frequencies are obtained from a damped harmonic oscillator fit of reflectivity spectra with a complex dielectric function $\varepsilon(\omega)$ in the factorized form (generalized Lyddane–Sachs–Teller relation) [10, 11]

$$\varepsilon(\omega) = \varepsilon_1(\omega) + \varepsilon_2(\omega) = \varepsilon_\infty \prod_{j=1}^{n} \frac{\Omega_{j\mathrm{LO}}^2 - \omega^2 - \mathrm{i}\gamma_{j\mathrm{LO}}\omega}{\Omega_{j\mathrm{TO}}^2 - \omega^2 - \mathrm{i}\gamma_{j\mathrm{TO}}\omega}, \tag{1}$$

where ε_∞ represents the high frequency dielectric constant (at frequencies large compared with the lattice vibration frequencies but small compared with the electronic transition frequencies), $\Omega_{j\mathrm{LO}}$ and $\Omega_{j\mathrm{TO}}$ are the longitudinal and transverse eigenfrequencies of the jth optical phonon mode, $\gamma_{j\mathrm{LO}}$ and $\gamma_{j\mathrm{TO}}$ represent their longitudinal and transverse damping constants. Using this dielectric function, all the reflectivity spectra in our measurements were fitted with the well known Fresnel formula for reflectivity of a half-space medium in vacuum [12]:

$$R(\omega) = \left| \frac{\sqrt{\varepsilon(\omega)} - 1}{\sqrt{\varepsilon(\omega)} + 1} \right|^2. \tag{2}$$

On the basis of equations (1) and (2), a fit of $R(w)$ to the observed reflectivity spectra can be obtained with a proper choice of the model parameters $\Omega_{j\mathrm{LO}}$, $\Omega_{j\mathrm{TO}}$, $\gamma_{j\mathrm{LO}}$, $\gamma_{j\mathrm{TO}}$ and ε_∞.

Table 1. The phonon parameters for the Lorentzian fits to the conductivity of $Dy_2Ti_2O_7$ single crystal at different temperatures. All units are in cm^{-1}.

Temperature, T (K)		F_{1u} modes							
300	Ω_{TO}	—	137	226	261	374	440	545	608
	γ_{TO}	—	23	77	44	62	26	36	18
	Ω_{LO}	—	143	253	320	437	537	608	745
	γ_{LO}	—	12	31	33	26	38	19	36
250	Ω_{TO}	—	133	224	261	372	442	544	611
	γ_{TO}	—	18	65	40	60	22	31	18
	Ω_{LO}	—	142	253	320	440	537	611	742
	γ_{LO}	—	13	29	31	22	33	19	26
200	Ω_{TO}	93	135	204	259	370	444.5	543	608
	γ_{TO}	15	23	62	26	42	16	23	17
	Ω_{LO}	93.5	144	254	322	443	538	608	746
	γ_{LO}	12	12	22	29	16	24	18	20
150	Ω_{TO}	91.5	130	199	259	370	447	544	608
	γ_{TO}	18	18	45	45	35	16	23	16.5
	Ω_{LO}	92	142	254	321	445	538	608	749
	γ_{LO}	14	13	20	29	16	25	17	28
100	Ω_{TO}	88	127	198	258	370	450	546	607
	γ_{TO}	18	12	36	20	33	19	29	20
	Ω_{LO}	90	140	252	320	447.5	537	607	748
	γ_{LO}	23	12	20	30	20	35	21	45
50	Ω_{TO}	86	127	197	259	370	453	545	612
	γ_{TO}	15	10	29	18	31	19	30	20
	Ω_{LO}	89	141	252	320	450	536	612	748
	γ_{LO}	29	15	18	28	20	34	21	45
10	Ω_{TO}	85	126	197	260	370	454	545	612
	γ_{TO}	15	7	26	17	27	18	31	22
	Ω_{LO}	90	139	253	317	451	535	612	748
	γ_{LO}	27	17	18	26	20	34	23	43

Adjustment of the parameters is done by trial and error fitting of formula (2) to the experimental spectra. This method yields not only $\varepsilon(\omega)$ but also the model parameters which characterize the infrared active phonons.

From a group theoretical analysis [13], a compound with the pyrochlore structure symmetry should have the vibrational phonon modes at the Brillouin zone centre Γ point with

$$\Gamma = 8F_{1u} + 4F_{2u} + 2F_{1g} + 4F_{2g} + 3E_u + E_g + A_{1g} + 3A_{2u}.$$

Among these 26 normal modes, only A_{1g}, E_g, $4F_{2g}$ are Raman active, $7F_{1u}$ are infrared active, and one F_{1u} acoustic. Consequently, the observed phonons in the spectra of $Dy_2Ti_2O_7$ at low temperature except that at about 610 cm^{-1} were denoted sequentially from low to high frequencies by F_{1u}^1 to F_{1u}^7. The number is in good agreement with the group theoretical analysis. The mode at 610 cm^{-1}, denoted by $F_{1u}{}^{7*}$, is weak in intensity and does not change with the temperature. It probably originates from two-phonon absorption because of its low intensity [14].

The fitting results for the oscillator parameters for all the phonon modes of $Dy_2Ti_2O_7$ are summarized in table 1. The high frequency dielectric constant is adopted as 5.0. Figure 2 shows the experimental and fitting curves at two representative temperatures of 300 and 10 K. The fitting results with the Lorentz oscillators could explain the global features of the phonon

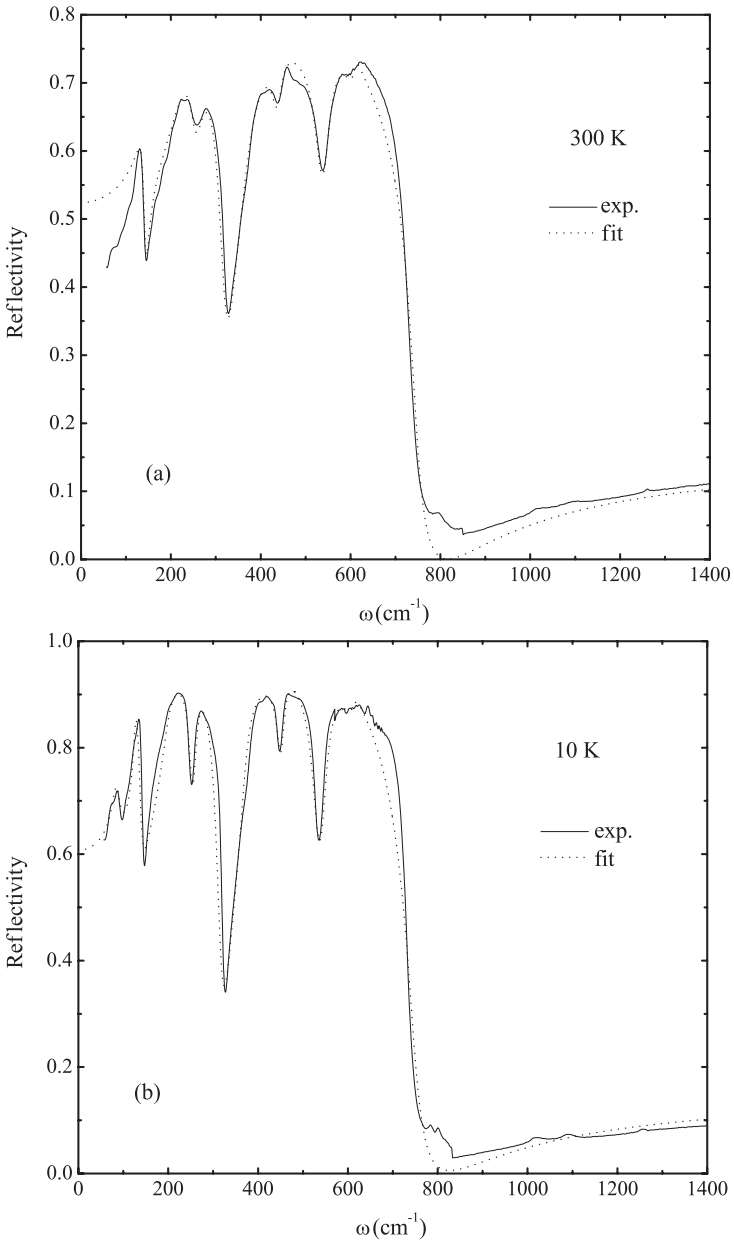

Figure 2. Representative experimental and fitted reflectivity spectra of $Dy_2Ti_2O_7$ at (a) 300 K and (b) 10 K. Solid lines represent experimental data and dotted lines are the fitting results.

spectra reasonably well, even though some difference between the experimental and the fitted data remains. A small deviation of the calculated curves from the experimental one is seen on the low frequency edge of the F^2_{1u} mode at high temperature. A possible reason is the reflection from the rear surface of the sample due to its transparency at low frequencies as well as the cut-off of the working frequency of the detector. However, the deviation has little impact on other phonon fitting parameters in other frequency ranges.

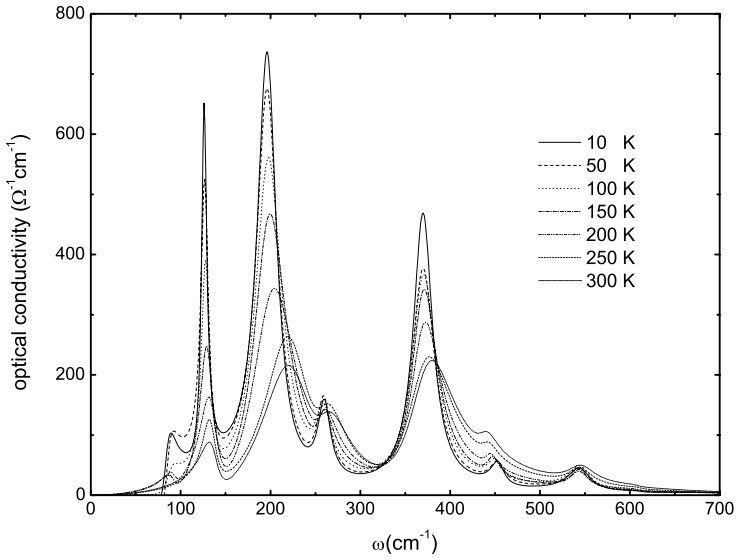

Figure 3. The real part of the temperature dependent optical conductivity of $Dy_2Ti_2O_7$ in the far infrared region.

The real part of the optical conductivity $\sigma_1(\omega)$ can be extracted from $\varepsilon_2(\omega)$, where $\sigma_1(\omega) = 1.6638 \times 10^{-2}\omega\varepsilon_2(\omega)$; here ω is in units of cm^{-1} and σ_1 in units of Ω^{-1} cm^{-1}. The corresponding result is shown in figure 3 [15]. The conductivity is dominated by seven peak structures due to optical phonon absorption; no free carrier contribution can be observed. For normal materials, with decreasing T, the anharmonic thermal motion would decrease, which results in a decrease in the lattice constant. Then the phonons should shift to higher frequencies and their linewidth should become narrower. The F^6_{1u} mode has clearly demonstrated this effect. Its centre frequency shifts from 439 to 452 cm^{-1} as the temperature decreases from 300 down to 10 K. Moreover, the phonon peak becomes more and more prominent and separated from the nearby mode F^5_{1u}. But it is puzzling that other modes do not exhibit the same behaviour; the three most prominent phonons, F^2_{1u}, F^3_{1u} and F^5_{1u}, show discernible redshifts. Coupling of phonons to magnetic excitations in solids may result in a change of phonon self-energy, i.e., the frequency due to spin–phonon interaction. Therefore, spin–phonon coupling [16] closely correlated with the Dy^{3+} (its effective spin $S = 1/2$) is a possible origin for the abnormal temperature dependence of the phonon frequency. As we mentioned in the introduction, Dy^{3+} cations can have appreciable magnetic moments. Consequently, ferromagnetic nearest neighbour dipole–dipole interactions will be present in spin ice $Dy_2Ti_2O_7$ in which large dipole interactions have been suggested to be responsible for the spin ice behaviour [17]. These effects have been quantitatively confirmed by both experimental and theoretical approaches [9]. At the nearest neighbouring sites, the exchange interactions between the magnetic atoms become the strongest. Subsequently, the crystal potential U can be described as follows:

$$U = \tfrac{1}{2}kx^2 + \sum_{ij} J_{ij}\langle S_i S_j\rangle, \tag{3}$$

where x is the atomic displacement from the equilibrium position in the oscillator model. In the second term, J_{ij} is the exchange energy constant which is a function of the structural parameters, such as the bond lengths between Dy^{3+} cations and the corresponding bond angles mediated by the O ions. S_i represents the spin of the Dy^{3+} cation at the i th site. $\langle S_i S_j\rangle$ denotes

a statistical average over the adjacent spins. The harmonic force constant derived from its second-derivative formula reads

$$\frac{\partial^2 U}{\partial x^2} = k + \sum_{ij}\left(\frac{\partial^2 J_{ij}}{\partial x^2}\right)\langle S_i S_j\rangle. \tag{4}$$

Note that the second term represents the spin–phonon coupling, which suggests that the phonon frequency should have an additional contribution. As for the spin–phonon coupling coefficient, $\sum_{ij}(\frac{\partial^2 J_{ij}}{\partial x^2})$ can be different for each phonon and can have either a positive or a negative sign. Furthermore, different phonon frequencies will have redshift or blueshift in the optical conductivity spectra. As the temperature decreases, the spin fluctuation becomes weaker and the spin–phonon coupling stronger. It is important to note that although ferromagnetic correlations are short ranged without long range order in spin ice compounds, from neutron scattering measurements Harris *et al* [18] have shown that the range of ferromagnetic order increases at lower temperature. As a result, the spin–phonon coupling range is wider so the phonon frequency shows a redshift or blueshift, which is in agreement with what is observed for our optical conductivity spectra.

Now we focus on the remarkable change of the spectral weight which is proportional to the area under the optical conductivity peak. It is well known that, on decreasing the temperature, the thermal fluctuation reduces, which may result in narrowing in the linewidth and enhancement in the oscillator strength without any changes in the bonding or coordination. Almost all phonon modes exhibit the theoretically predicted behaviour in our optical conductivity spectra. But the spectral weight should not change. The anomalous increase in oscillator strength of the low frequency modes must be taken care of. Optical sum rules provide a powerful tool with which to analyse the behaviour of free carriers and bound excitations [19]. The partial conductivity sum rules corresponding primarily to a single class of absorption such as excitation of phonons or conduction, valence or core electrons have been developed. For oscillator states, the partial conductivity sum rule can be expressed as [20]

$$\frac{120}{\pi}\int_{\omega_a}^{\omega_b}\sigma_1(\omega)\,\mathrm{d}\omega = \omega_{p,j}^2, \tag{5}$$

where ω_a, ω_b and $\omega_{p,j}$ (in units of cm^{-1}) are the integral lower and upper limits and effective plasma frequency associated with the isolated phonon absorption, respectively. In the above equation, σ is in units of $\Omega^{-1}\,\mathrm{cm}^{-1}$. The integral region of the jth oscillator should be chosen to cover the full spectral weight. The dramatic increase in the spectral weight has implications for the distribution of charge and the change in local strength of the binding charge. The effective charge of Dy, Ti and O ions in the unit cell with k atoms can be determined through the following equation (6) (in the Gauss unit system) [21]:

$$\frac{1}{\varepsilon_\infty}\sum_j \omega_{p,j}^2 = \frac{4\pi}{V_\mathrm{c}}\sum_k \frac{(Z_k^* e)^2}{M_k}, \tag{6}$$

where V_c is the unit cell volume, j and k index the lattice modes and the atoms with mass M_k, respectively. For the effective charge, there is a general expression $\sum_k Z_k^* = 0$.

In $Dy_2Ti_2O_7$, oxygen is the lightest element; therefore, in the right-hand side of equation (6), the summation is dominated by the O ion term and the terms for Dy ions and Ti ions may be neglected. The change in the effective charge is associated mainly with the oxygen (i.e., $Z_k^* \approx Z_\mathrm{O}^*$). Combining equations (5) and (6), we obtain the value for Z_O^* as shown in figure 4. The absolute value of Z_O^* is of less significance; what is important is the temperature dependence of the deduced value for Z_O^*, which increases with decreasing temperature. When the incident light couples to the induced dipole moments created by the atomic displacements

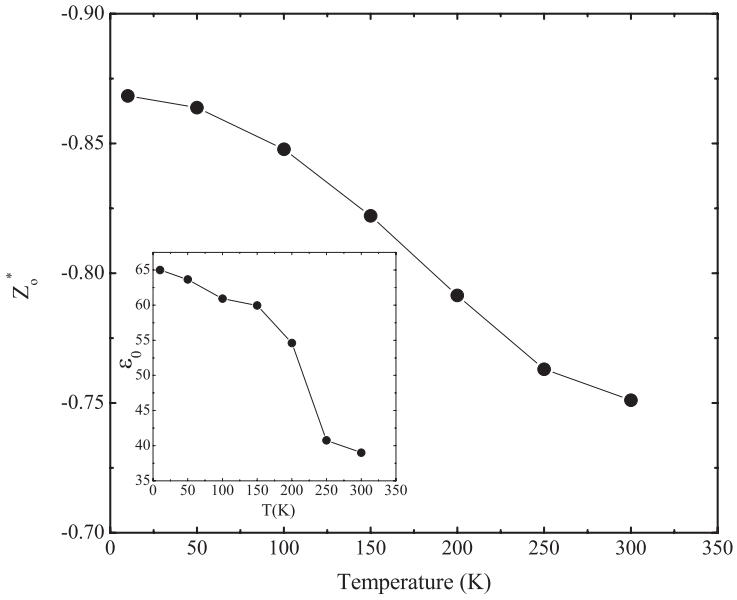

Figure 4. The temperature dependence of the Born effective charge per oxygen atom in $Dy_2Ti_2O_7$. The dots represent the values deduced at various temperatures between 300 and 10 K. Inset: the temperature dependence of the static optical permittivities.

associated with a normal mode, if the Born effective charge per oxygen atom Z^*_O is increasing, then the size of the induced dipole moment and the optical absorption will also increase, which explains well the above temperature dependence of the optical conductivity. On the other hand, the increase in Z^*_O means a change in the bond length and bond angle between O ion and cations, so the bond lengths between Dy^{3+} cations and the corresponding bond angles mediated by the O ions will change. Subsequently, J_{ij} and $\langle S_i S_j \rangle$ have different changes associated with the phonon central frequency shift as we observed above. In summary, the change in the effective charge arising from electrical charge localization strengthening is the fundamental reason that the spectral weight increases and the phonon frequency shifts. From our experimental results, within the framework of the ferromagnetic spin ice model, we consider that the increase in Z^*_O is closely related to the nearest neighbour ferromagnetic interaction strengthening and/or widening in the correlation range. In this simple physical picture, the increasing FM exchange between Dy^{3+} cations will lead to a decrease of the distance between mediated O ions and Dy^{3+}, which enhance the increase in Z^*_O, in agreement with our experimental observation.

The LST relationship also provides an effective examination of static optical permittivities ε_0 in the approximation of zero phonon frequency. When $\omega = 0$, the equation evolves into the following form:

$$\frac{\varepsilon_0}{\varepsilon_\infty} = \prod_i \frac{\Omega^2_{i\mathrm{LO}}}{\Omega^2_{i\mathrm{TO}}}. \tag{7}$$

From equation (7), ε_0 for $Dy_2Ti_2O_7$ single crystal at different temperatures is also obtained, as shown in the inset of figure 4. It exhibits the same temperature dependence as Z^*_O, which suggests that the temperature dependence of ε_0 could originate from that of Z^*_O and, essentially, charge localization arising from FM exchange plays an important role in the temperature variations of both ε_0 and Z^*_O.

4. Conclusions

In conclusion, the FIR response of $Dy_2Ti_2O_7$ single crystals has been studied at different temperatures. Seven infrared active phonons have been observed, which agrees well with a group analysis. All the spectra are fitted with the oscillator model and an excellent agreement between experimental and calculated spectra is obtained. Of the phonons, one shows a discernible blueshift and three obvious redshifts with decreasing temperature. The shifts are attributed to the spin–phonon coupling in a geometrically frustrated configuration in the spin ice material. The oscillation strengths of the low frequency modes increase dramatically at low temperature, indicating that the Born effective charges are increasing in the unit cell. We propose that the temperature dependence of the static optical permittivity being similar to that of the Born effective charge may originate from the intrinsic charge localization resulting from the nearest neighbour FM interaction.

Acknowledgments

This work was supported by the National Science Foundation of China (Grants Nos 10474128 and 10474074).

References

[1] Ramirez A P, Hayashi A, Cava R J, Siddharthan R and Shastry B S 1999 *Nature* **399** 333
[2] Snyder J, Ueland B G, Slusky J S, Karunadasa H, Cava R J and Schiffer P 2004 *Phys. Rev.* B **69** 064414
[3] Snyder J, Slusky J S, Cava R J and Schiffer P 2001 *Nature* **413** 48
[4] Fennell T, Petrenko O A, Balakrishnan G, Bramwell S T, Champion J D M, Fak B, Harris M J and Paul D M 2002 *Appl. Phys.* A **74** S889
[5] Higashinaka R, Fukazawa H and Maeno Y 2003 *Phys. Rev.* B **68** 014415
[6] Matsuhira K, Hinatsu Y and Sakakibara T 2001 *J. Phys.: Condens. Matter* **13** L737
[7] Melko R G, den Hertog B C and Gingras M J P 2001 *Phys. Rev. Lett.* **87** 067203
[8] Yoshida S, Nemoto K and Wada K 2004 *J. Phys. Soc. Japan* **71** 1619
[9] Fukazawa H, Melko R G, Higashinaka R, Maeno Y and Gingras M 2002 *Phys. Rev.* B **65** 054410
[10] Gervais F 1983 *Infrared and Millimetre Waves* vol 8, ed K J Button (New York: Academic) p 279
[11] Massa N E, Campa J and Rasines I 1995 *Phys. Rev.* B **52** 15920
[12] Tajima S, Ido T, Ishibashi S, Itoh T, Eisaki H, Mizuo Y, Arima T, Takagi H and Uchida S 1991 *Phys. Rev.* B **43** 10496
[13] Fateley W G, Dollish F R, McDevitt N T and Bentley F F 1972 *Infrared and Raman Selection Rules for Molecular and Lattice Vibrations: The Correlation Method* (New York: Wiley–Interscience)
[14] Kamba S, Buixaderas E and Pajaczkowska A 1998 *Phys. Status Solidi* a **168** 317
[15] Bruesch P 1986 *Phonons: Theory and Experiments II* (Berlin: Springer) chapter 2, p 14
[16] Lee J S, Noh T W, Bae J S, Yang I-S, Takeda T and Kanno R 2004 *Phys. Rev.* B **69** 214428
[17] den Hertog B C and Gingras M J P 2000 *Phys. Rev. Lett.* **84** 3430
[18] Harris M J, Bramwell S T, McMorrow D F, Zeiske T and Godfrey K W 2000 *Phys. Rev. Lett.* **79** 2554
[19] Smith D Y 1985 *Handbook of Optical Constants of Solids* (New York: Academic)
[20] Homes C C, Vogt T, Shapiro S M, Wakimoto S, Subramanian M A and Ramirez A P 2003 *Phys. Rev.* B **67** 092106
[21] Scott J F 1997 *Phys. Rev.* B **4** 1360